

# Low invasive multisensor acquisition system for real-time monitoring of cardiovascular and respiratory parameters

Riccardo Pernice  
Department of Engineering  
University of Palermo  
Palermo, Italy  
[riccardo.pernice@unipa.it](mailto:riccardo.pernice@unipa.it)

Antonino Parisi  
Department of Engineering  
University of Palermo  
Palermo, Italy  
[antonino.paris@unipa.it](mailto:antonino.paris@unipa.it)

Saverio Guarino  
Department of Engineering  
University of Palermo  
Palermo, Italy  
[saverio.guarino@virgilio.it](mailto:saverio.guarino@virgilio.it)

Giorgio Fallica  
STMicroelectronics  
Catania, Italy  
[piero.fallica@gmail.com](mailto:piero.fallica@gmail.com)

Vincenzo Vinciguerra  
STMicroelectronics  
Catania, Italy  
[vincenzo.vinciguerra@st.com](mailto:vincenzo.vinciguerra@st.com)

Giuseppe Ferla  
STMicroelectronics  
Catania, Italy  
[pino.ferla@gmail.com](mailto:pino.ferla@gmail.com)

Luca Faes  
Department of Engineering  
University of Palermo  
Palermo, Italy  
[luca.faes@unipa.it](mailto:luca.faes@unipa.it)

Alessandro Busacca  
Department of Engineering  
University of Palermo  
Palermo, Italy  
[alessandro.busacca@unipa.it](mailto:alessandro.busacca@unipa.it)

**Abstract**— The recent advances in multiparametric monitoring of biosignals and management of big data prompt for the development of devices and techniques for the extraction of indicators with physiological relevance. In this context, we have designed and realized a portable electronic system, equipped with simple biomedical sensors, able to synchronously record multiple electrocardiographic (ECG), photoplethysmographic (PPG) and breathing signals, for carrying out a non-invasive monitoring of several cardiovascular parameters. In this work, we show the results of preliminary measurements performed following a specific physiological protocol (i.e., deep breathing with 10 s per cycle). The system allows to monitor specific physiological behaviors, such as the decrease of the R-R interval (increase of the heart rate) during inhalation and the increase of the stroke volume increases during exhalation. The high quality of the ECG/PPG/breath waveforms acquired by our probes, sensors and system allows an improvement in the accuracy of the extraction of noteworthy cardiovascular parameters.

**Keywords**— Wearable electronics, portable system, electrocardiography (ECG); photoplethysmography (PPG), heart rate variability

## I. INTRODUCTION

Real time acquisition and monitoring of biomedical parameters for early disease detection is becoming more and more widespread in daily life [1]–[3], thanks to the development of minimally invasive portable or wearable devices [4]–[7]. The recent spread of Internet of Things (IoT) approach, which can be defined as a network of devices interacting with each other via machine to machine (M2M) communications allowing acquisition and transfer of a lot of data, has recently been the focus of several research works, and can be considered as a potential solution to alleviate the pressures on healthcare systems [8]–[10]. In the field of healthcare, the IoT approach is typically pursued through the development of networks of sensors (especially wearable) for the recording of medical/vital parameters for various purposes, e.g. monitoring, rehabilitation and ambient assisted

living (AAL) for elderly people [8]. Wearable devices acquire large amount of data and employ suitable algorithms to identify patterns, to detect early stages of chronic diseases often before the insurgence of symptoms [11]. Moreover, the involvement of high-tech big companies (e.g. Apple, Fitbit, Xiaomi, Huawei, Garmin) in the development and commercialization of smartwatches and smartbands with several healthcare-related capabilities surely represents a boost for the research in this field [11].

Heart diseases have become one of the leading causes of death [2] and, according to the World Health Organization (WHO), heart disease rate might increase up to 23.3% worldwide by 2030 [12], with an annual cardiovascular disease mortality which is forecasted to increase from 17.5 million in 2012 to 22.2 million in 2030 [13]. This will be mainly due to the demographic shift towards an older population [14] and to the increased risk factors, such as unhealthy diet, high cholesterol, tobacco or alcohol addiction, high blood pressure [12], [14]. For this reason, performing a continuous self-monitoring of cardiovascular parameters is crucial not only for a timely detection of ongoing diseases, but also for reducing the risk of insurgence of cardiac pathologies. Some of the main vital parameters that should be carefully monitored to assess health conditions of the patient include heart rate and its variability [15], blood pressure, and respiratory rate. In order to perform real-time physiological monitoring, it is possible to exploit photoplethysmography (PPG), which is a low-cost, easy-to-use and unobtrusive optical technique widely used to detect microvascular blood volume changes in tissues, either in reflection or transmission mode [6], [16]–[18]. The working principle of PPG relies on the fact that blood absorbs infrared light more than the remaining skin tissues [14]. PPG has become widespread, being now even employed in smartphones and smartwatches [19]–[21]. A wide range of physiological parameters can be extracted using PPG, e.g., heart rate, heart rate variability, oxygen saturation, pulse-transit time, blood pressure

estimation (refer to [15], [16], [18], [22]–[24] for further information).

In our previous works ([6], [7], [25], [26]), we demonstrated the effectiveness of an embedded portable system to carry out synchronous electrocardiographic (ECG) and PPG measurements. In particular, in [6] we showed the capability of extracting heart and breath rate, pulse arrival time, pulse transit time and pulse wave velocity (we refer to [24], [27] for further details) and also of estimating blood pressure, while in [25] we described a more advanced version of the combo system supporting a higher number of channels also discussing different algorithms to obtain the pulse-to-pulse interval for calculating the heart rate and the heart rate variability. In this work, we add the capability to acquire a respiratory signal to perform synchronous ECG/PPG/breath signal acquisitions. The aim is to realize a device capable of carrying out real-time continuous monitoring of multiple physiological parameters, in a non-invasive manner. In this paper, we show the effects of deep breathing on photoplethysmographic waveforms, since it has been demonstrated that deep breathing produces strong effects on heart rate and blood pressure [28]–[31]. The preliminary results are promising.

## II. MATERIALS AND METHODS

### A. Experimental set-up

Measurements have been carried out using a more advanced version of our embedded portable system now capable of synchronous acquisition of multiple ECG/PPG/breathing signals. A schematic diagram and a photo of the system are shown in Fig. 1(a) and (b), respectively.

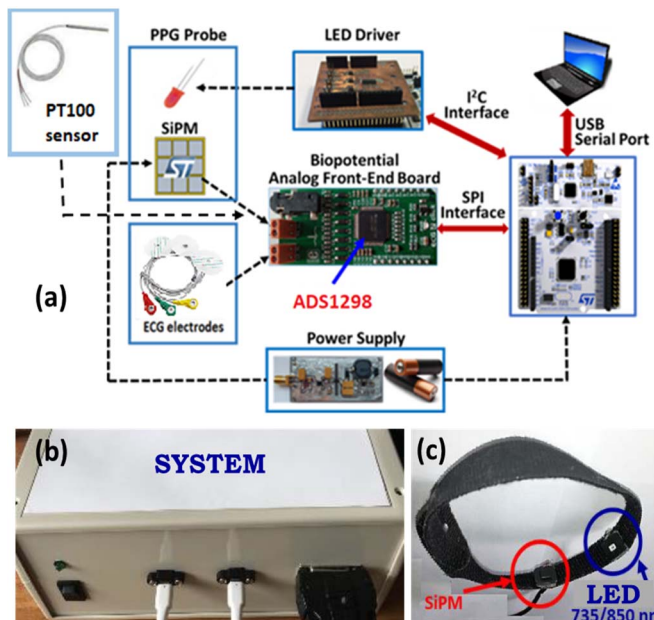


Fig. 1. (a) Schematic block diagram and (b) photograph of our system and (c) photo of a PPG probe.

The system includes: (i) a Texas Instruments ADS1298 analog front-end (AFE) for biopotential measurements, supporting up to 8 channels with 24-bit resolution, 1 kHz sampling rate (ii) a current LED driver, (iii) an STM32-F401RE microcontroller integrated within a NUCLEO-F401 development board to manage the AFE and (iv) a battery-

operated power supply. The current implementation of the system supports the acquisition of up to 3 ECG leads, 2 PPG waveforms and 1 breath signal. Standard commercial disposable adhesive electrodes were used to obtain ECG recordings. In order to acquire PPG waveforms, we have developed probes (shown in Fig.1(c)) composed of LEDs emitting at 735 and 850 nm and of a Silicon Photomultiplier (SiPM) detector (provided by STMicroelectronics) with high responsivity and gain. Further information on SiPMs, their characterization and applications can be found in [7], [32]–[34]. The use of SiPMs as detectors and the synchronous acquisition of multiple ECG/PPG/breath signals with a single device with 24-bit resolution represent the most innovative aspects of our work. Moreover, the system is equipped with an appositely developed Graphical User Interface which plots and save in real time the acquired signal and visualizes useful cardiovascular parameters (see [25] for further details). Finally, we have employed a thin film temperature sensor, PT100 Class A with 0.1 s thermal response time in flowing air, to obtain the breathing signal.

### B. Measurement protocol

In this work, ECG, PPG and breath signals were synchronously acquired with a sampling frequency of 1 kHz. ECG data consisted of 3-lead electrocardiographic signals, with electrodes positioned on both the left and right arms and legs (standard Einthoven's triangle). PPG signals were recorded on the left and on the right wrist. Finally, a breathing flow signal was acquired measuring the temperature variations during breath (i.e., inhalation and exhalation phases) employing the PT100 sensor placed near the volunteer's nose.

Preliminary measurements herein described were carried out on a healthy male subject, 77 years old, using a 10-second deep breathing protocol which includes the following phases: (a) inhalation: 4 s; (b) rest: 1 s; (c) exhalation: 4 s; (d) rest: 1 s. In order to carry out a controlled breathing mechanism aimed at having a constant pressure on the lungs, a 25-cm long straw with a diameter of 4 mm was used during breathing. The pressure during the expiration has been estimated equal to 80 mm H<sub>2</sub>O.

A metronome-like application (shown in Fig. 2) which visually displays the current phase and a moving bar illustrating the remaining time to the following phase, was developed to allow the volunteer to properly follow the protocol for 8 minutes.



Fig. 2. (a) Screenshot of the metronome application during (a) inhalation phase; (b) rest and (c) exhalation phase.

The combined employment of our system, the PT100 sensor and the metronome application has allowed us to acquire breathing signals with well-defined phases (i.e., inhalation, rest and exhalation), as shown in Fig. 3. As reported, during inhalation (red) the temperature recorded by the sensor decreases, while during the exhalation (green) it

instead increases; finally, during resting periods (grey) the temperature tends to the mean value.

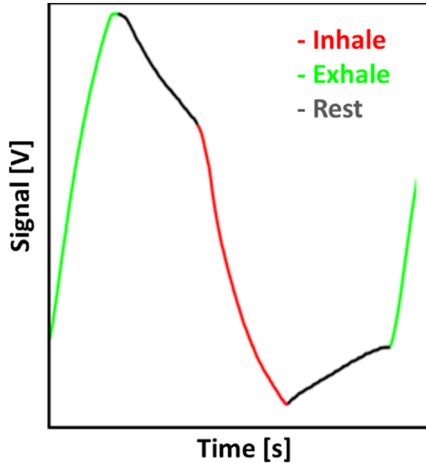


Fig. 3. Example of breathing signal obtained during deep breathing.

### C. Data analysis

In order to improve signal quality and reduce noise, all the acquired waveforms were preprocessed using suitable digital filters. For ECG signals, a zero-phase 4<sup>th</sup> order band-pass Butterworth digital filter was employed, with low and high cut-off frequencies equal to 0.1 Hz and 20 Hz, respectively, in order to both remove the baseline wander and the 50 Hz power-line frequency. The raw PPG data were already of sufficiently good quality, thanks to the employment of SiPMs and to the 24-bit resolution of our acquisition system which reduces the noise. For this reason, a simple low-pass moving average filter (smoothing) with a time span of 11 points ( $\sim 1/100$  sampling frequency) was employed. The moving average filter was also applied to the breathing signal, but in this case using a time span of 31 points ( $\sim 1/30$  sampling frequency). The employed filters are zero-phase and do not introduce delays between the signals.

Starting from the acquired data, after employing the Pan-Tompkins algorithm to extract QRS complexes [35], the  $n$ -th RR interval (RRI) was calculated from the ECG as the time interval between the  $n$ -th and  $(n+1)$ -th QRS apexes [22], [23]. Instead, the  $n$ -th pulse-to-pulse interval (PPI) was measured as the time interval between the  $n$ -th and  $(n+1)$ -th PPG maxima, employing a threshold-based peak detection algorithm [25]. Finally, the Pulse Arrival Time (PAT) between the heart and the wrist was calculated for each cardiac cycle as the time interval between the ECG R peak and the corresponding maximum value of the PPG waveform [36].

## III. RESULTS AND DISCUSSION

Figure 4 depicts a 15-second synchronous recording of the ECG Lead I track, of the right wrist PPG waveform and of the breathing signal.

Figure 4(b) demonstrates the good quality of morphological features of the PPG signal acquired using our probes, sensors and system, thanks to the increased signal-to-noise ratio (around 50 dB) and relatively high AC/DC ratio (around 1/12). The envelope of the average PPG waveform represents the modulation due to breathing. For better clarity, in the figure the breathing signal is inverted. The red line represents the inhalation phase, the green line the exhalation, while grey zones the resting periods. The PPG signal shown

in Fig. 4(c) is obtained removing the modulation due to breathing, employing a [0.3-15 Hz] band-pass filter. The stroke volume has been estimated as the area under the PPG curve for each cardiac cycle [37], [38]. The stroke volume trend is shown in red. Analysis clearly demonstrates that stroke volume increases during exhale and decreases in the inhale phase, with a delay of a few beats. The high quality of our signals allows the variations in the morphology of PPG waveforms to be easily highlighted, e.g. the diastolic notch becomes less visible (or even disappears) during inhalation.

Figure 5 shows 300-beats RRI time series extracted from ECG Lead I signal. As reported, apart from an ectopic beat detected at beat number 163, the time series follows the breathing rhythm (which is the well-known respiratory sinus arrhythmia [15], [39]). In detail, in the literature it has been demonstrated that RRI decreases (and thus the heart rate increases) during inspiration and instead increases (i.e., decreased heart rate) during expiration, i.e. the so-called Respiratory Sinus Arrhythmia (RSA) [39], [40]. As shown in the figure, such phenomenon is not immediately observed during deep breathing and a delay of a few beats has been recorded for each cycle. The average RRI recorded in the analysed measure is 533 ms, corresponding to a heart rate of 113 bpm.

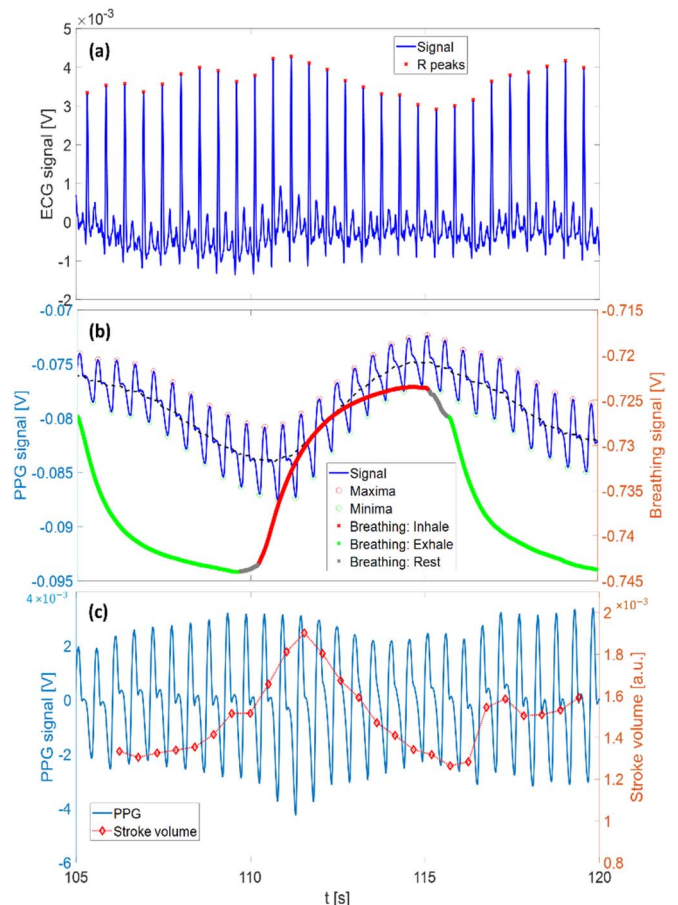


Fig. 4. Example of 15-second recording of (a) ECG Lead I, (b) right wrist PPG and breathing signal, and (c) estimated stroke volume. In (a) red crosses indicate R peaks. In (b) red circles denote PPG maxima, green ones PPG minima; the grey dotted line indicates the modulation due to the breathing. For the breathing signal, the red line indicates inhalation phase, green lines the exhalation, grey zones the resting periods. PPG signal in (c) is obtained

removing the modulation due to breathing. The connected red diamonds indicate the stroke volume.

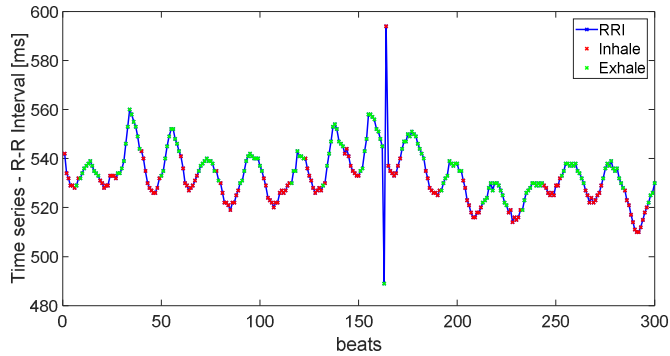


Fig. 5. RRI time series extracted from ECG Lead I signal. Red (green) markers represent points recorded during inhalation (exhalation) phase.

Figure 6 depicts the difference between the maxima and minima of the PPG signal during a 110-s time interval. We indicate with different colours the points recorded during inhalation and those during exhalation. As known in the literature, the difference between PPG maxima and minima represents the so-called systolic amplitude [41], [42]. Our results demonstrate that the systolic amplitude follows almost exactly the breathing rhythm, decreasing during inhalation and increasing during exhalation. It is also worth noting that the delay observed for RRI in this case is lower or even not observed in most cardiac cycles. The trends depicted in the figure can be explained by the fact that during exhalation the blood volume brought by veins to the left atrium is higher, with augmented stroke volume, followed by an increase of the systolic pressure; the opposite phenomena are observed during inhalation. The effects are more evident during deep breathing, and this may be related to the widely known fact that deep breathing produces noteworthy consequences on heart rate, stroke volume and blood pressure [28]–[31].

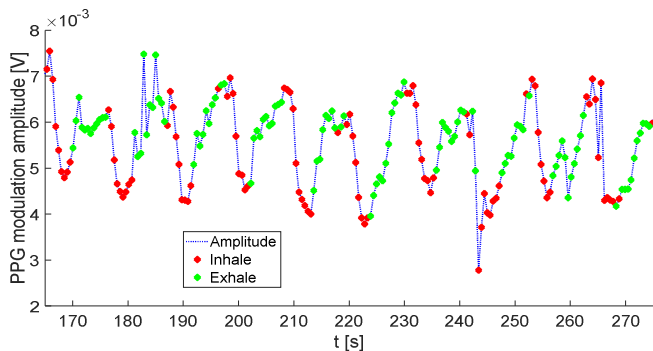


Fig. 6. (a) Difference between maxima and minima of PPG signal over the entire measurement timespan (110-s window). Red (green) markers represent points recorded during inhalation (exhalation) phase.

Figure 7 shows the trend of the Pulse Arrival Time during a 200-s interval. As reported, also in this case the physiological parameter follows the breathing rhythm, decreasing during exhalation and increasing during inhalation, but with a delay of a few beats per cycle. In this case, a plausible reason for the observed discrepancies can be related to the distorting effect of non-constant pre-ejection period (PEP) which has been shown to exhibit physiological variability [23], [24]. The average measured PAT is 278 ms.

The results herein illustrated are reproducible for the whole measurement duration and on different volunteers.

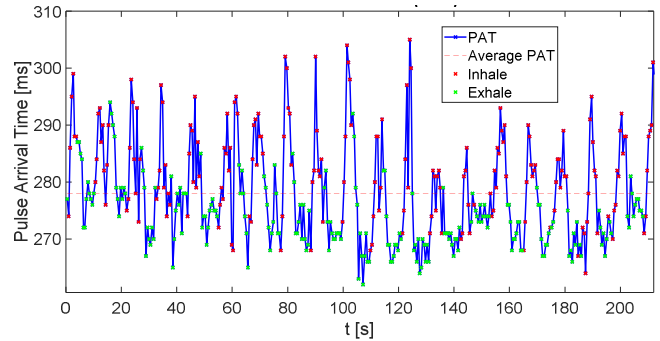


Fig. 7. PAT calculated as the time interval between ECG R-peaks and PPG maxima. Red (green) markers represent points recorded during inhalation (exhalation) phase.

#### IV. CONCLUSION

Our analysis demonstrates the effectiveness of our combo embedded system to carry out synchronous ECG/PPG/breath measurements. Results indicate that the employment of SiPMs as photodetectors in the PPG probes and the 24-bit resolution strongly reduce noise, permitting the acquisition of good quality waveforms, with high AC/DC ratio. The employment of a PT100 sensor in our system has allowed the acquisition of a signal proportional to breathing, also synchronized with ECG and PPG waveforms. Preliminary ECG/PPG/breath analysis during deep breathing controlled via a metronome-like application was aimed at better understanding the behaviour of main physiological parameters in the inhalation/exhalation phases. Our results highlight that during exhalation the PAT decreases, while RRI and the PPG systolic amplitude increase, indicating a rise of stroke volume, while the opposite is observed during inhalation. The parameters calculated using our system are of fundamental physiological importance, e.g. the PAT can be considered a marker for blood pressure [43], and can be extracted only combining different biosignals acquired synchronously at different body locations.

In conclusion, the obtained results can lead to the development of a single device able to perform real-time continuous and non-invasive monitoring of multiple physiological parameters, including blood pressure, for early disease diagnosis. The developed system thus represents a useful tool for e-health and smart healthcare, and can be used for various purposes, such as monitoring of healthy people or of subjects potentially at risk of cardiovascular diseases, but also for rehabilitation and in ambient assisted living environments.

Further measurements are currently underway to confirm such preliminary results. Future steps will include multiple PPG measurements on other body parts (e.g., ankle, carotid) are also planned, still combined with ECG tracks. Combining all such signals recorded on different sites and for long period of times using this low-invasive wearable system and analyzing them with advanced multiparametric biosignal processing techniques well fits IoT approach and will surely be exploited in the future for everyday life in different environments (e.g., home, workplace, automotive).

## ACKNOWLEDGMENT

Research supported by PON R&I 2014-2020 AIM project no. AIM1851228-2, grant no. 692470 - ASTONISH Project, H2020-EU.2.1.1.7. – ECSEL, and PRIN 2017, PRJ-0167, “Stochastic forecasting in complex systems”, University of Palermo, Italy.

## REFERENCES

- [1] O. S. Alwan and K. P. Rao, “Dedicated real-time monitoring system for health care using ZigBee,” *Healthc. Technol. Lett.*, vol. 4, no. 4, pp. 142–144, 2017.
- [2] P. Kakria, N. Tripathi, and P. Kitipawong, *A Real-Time Health Monitoring System for Remote Cardiac Patients Using Smartphone and Wearable Sensors*, vol. 2015, 2015.
- [3] M. M. Baig, H. GholamHosseini, A. A. Moqem, F. Mirza, and M. Lindén, “A systematic review of wearable patient monitoring systems—current challenges and opportunities for clinical adoption,” *J. Med. Syst.*, vol. 41, no. 7, p. 115, 2017.
- [4] D. Hernando, S. Roca, J. Sancho, Á. Alesanco, and R. Bailón, “Validation of the Apple Watch for Heart Rate Variability Measurements during Relax and Mental Stress in Healthy Subjects,” *Sensors*, vol. 18, no. 8, 2018.
- [5] M. Zanetti *et al.*, “Information Dynamics of the Brain, Cardiovascular and Respiratory Network during Different Levels of Mental Stress,” *Entropy*, vol. 21, no. 3, 2019.
- [6] D. Oreggia *et al.*, “Physiological parameters measurements in a cardiac cycle via a combo PPG-ECG system,” in *2015 AEIT International Annual Conference (AEIT)*, 2015, pp. 1–6.
- [7] V. Vinciguerra *et al.*, “PPG/ECG Multisite Combo System Based on SiPM Technology,” in *Sensors. CNS 2018. Lecture Notes in Electrical Engineering book series (LNEE)*, vol. 539, Andò B. *et al.* (eds), Ed. Springer, Cham, 2019, pp. 353–360.
- [8] S. B. Baker, W. Xiang, and I. Atkinson, “Internet of things for smart healthcare: Technologies, challenges, and opportunities,” *IEEE Access*, vol. 5, pp. 26521–26544, 2017.
- [9] Y. I. N. Yuehong, Y. Zeng, X. Chen, and Y. Fan, “The internet of things in healthcare: An overview,” *J. Ind. Inf. Integr.*, vol. 1, pp. 3–13, 2016.
- [10] S. Sarkar and S. Misra, “From micro to nano: The evolution of wireless sensor-based health care,” *IEEE Pulse*, vol. 7, no. 1, pp. 21–25, 2016.
- [11] N. Chen, “Use of wearables for health management in the aging population,” 2019.
- [12] W. H. Organization, “Global status report on noncommunicable diseases 2010. Geneva: WHO,” 2011.
- [13] W. H. Organization, “Global status report on noncommunicable diseases 2014,” 2014.
- [14] M. C. Odden, P. G. Coxson, A. Moran, J. M. Lightwood, L. Goldman, and K. Bibbins-Domingo, “The impact of the aging population on coronary heart disease in the United States,” *Am. J. Med.*, vol. 124, no. 9, pp. 827–33.e5, Sep. 2011.
- [15] F. Shaffer and J. P. Ginsberg, “An Overview of Heart Rate Variability Metrics and Norms,” *Front. public Heal.*, vol. 5, p. 258, Sep. 2017.
- [16] J. Allen, “Photoplethysmography and its application in clinical physiological measurement,” *Physiol. Meas.*, vol. 28, no. 3, p. R1, 2007.
- [17] D. Agrò *et al.*, “PPG embedded system for blood pressure monitoring,” in *2014 AEIT Annual Conference - From Research to Industry: The Need for a More Effective Technology Transfer (AEIT)*, 2014, pp. 1–6.
- [18] Y. Sun and N. Thakor, “Photoplethysmography Revisited: From Contact to Noncontact, From Point to Imaging,” *IEEE Trans. Biomed. Eng.*, vol. 63, no. 3, pp. 463–477, 2016.
- [19] A. Bánhalmi, J. Borbás, M. Fidrich, V. Bilicki, Z. Gingl, and L. Rudas, “Analysis of a Pulse Rate Variability Measurement Using a Smartphone Camera,” *J. Healthc. Eng.*, vol. 2018, 2018.
- [20] S. A. Siddiqui, Y. Zhang, Z. Feng, and A. Kos, “A pulse rate estimation algorithm using PPG and smartphone camera,” *J. Med. Syst.*, vol. 40, no. 5, p. 126, 2016.
- [21] D. Biswas, N. Simões-Capela, C. Van Hoof, and N. Van Helleputte, “Heart Rate Estimation From Wrist-Worn Photoplethysmography: A Review,” *IEEE Sens. J.*, vol. 19, no. 16, pp. 6560–6570, 2019.
- [22] R. Pernice *et al.*, “Reliability of Short-Term Heart Rate Variability Indexes Assessed through Photoplethysmography,” in *2018 40th Annual International Conference of the IEEE Engineering in Medicine and Biology Society (EMBC)*, 2018, pp. 5610–5613.
- [23] R. Pernice *et al.*, “Comparison of short-term heart rate variability indexes evaluated through electrocardiographic and continuous blood pressure monitoring,” *Med. Biol. Eng. Comput.*, vol. 57, no. 6, pp. 1247–1263, 2019.
- [24] M. Gao, N. B. Olivier, and R. Mukkamala, “Comparison of noninvasive pulse transit time estimates as markers of blood pressure using invasive pulse transit time measurements as a reference,” *Physiol. Rep.*, vol. 4, no. 10, p. e12768, May 2016.
- [25] R. Pernice, A. Parisi, G. Adamo, S. Guarino, L. Faes, and A. Busacca, “A portable system for multiple parameters monitoring: towards assessment of health conditions and stress level in the automotive field,” in *2019 AEIT International Conference of Electrical and Electronic Technologies for Automotive (AEIT AUTOMOTIVE)*, 2019, pp. 1–6.
- [26] V. Vinciguerra *et al.*, “Progresses towards a processing pipeline in photoplethysmogram (PPG) based on SiPMs,” in *Circuit Theory and Design (ECCTD), 2017 European Conference on*, 2017, pp. 1–5.
- [27] E. von Wowern, G. Östling, P. M. Nilsson, and P. Olofsson, “Digital Photoplethysmography for Assessment of Arterial Stiffness: Repeatability and Comparison with Applanation Tonometry,” *PLoS One*, vol. 10, no. 8, pp. e0135659–e0135659, Aug. 2015.
- [28] N. Herakova, N. H. N. Nwobodo, Y. Wang, F. Chen, and D. Zheng, “Effect of respiratory pattern on automated clinical blood pressure measurement: an observational study with normotensive subjects,” *Clin. Hypertens.*, vol. 23, p. 15, Jul. 2017.
- [29] H. Mori *et al.*, “How does deep breathing affect office blood pressure and pulse rate?,” *Hypertens. Res.*, vol. 28, no. 6, p. 499, 2005.
- [30] M. A. Russo, D. M. Santarelli, and D. O’Rourke, “The physiological effects of slow breathing in the healthy human,” *Breathe (Sheffield, England)*, vol. 13, no. 4, pp. 298–309, Dec. 2017.
- [31] A. C. Dornhorst, P. Howard, and G. L. Leathart, “Respiratory variations in blood pressure,” *Circulation*, vol. 6, no. 4, pp. 553–558, 1952.
- [32] G. Adamo *et al.*, “Measurements of Silicon Photomultipliers Responsivity in Continuous Wave Regime,” *IEEE Trans. Electron Devices*, vol. 60, no. 11, pp. 3718–3725, 2013.
- [33] G. Adamo *et al.*, “Signal to Noise Ratio of silicon photomultipliers measured in the continuous wave regime,” in *2014 Third Mediterranean Photonics Conference*, 2014, pp. 1–3.
- [34] E. Sciacca *et al.*, “Silicon planar technology for single-photon optical detectors,” *IEEE Trans. Electron Devices*, vol. 50, no. 4, pp. 918–925, 2003.
- [35] J. Pan and W. J. Tompkins, “A Real-Time QRS Detection Algorithm,” *IEEE Trans. Biomed. Eng.*, vol. BME-32, no. 3, pp. 230–236, 1985.
- [36] S. Rajala, T. Ahmaniemi, H. Lindholm, and T. Taipalus, “Pulse arrival time (PAT) measurement based on arm ECG and finger PPG signals - comparison of PPG feature detection methods for PAT calculation,” in *2017 39th Annual International Conference of the IEEE Engineering in Medicine and Biology Society (EMBC)*, 2017, pp. 250–253.
- [37] N. Daimiwal and M. Sundhararajan, “Non Invasive Measurement and Analysis of Cardiac Output for Different Age Group using PPG Sensor,” *Int. J. Comput. Appl.*, vol. 975, p. 8887.
- [38] A. Vakily, H. Parsaei, M. M. Movahhedi, and M. A. Sahmeddini, “A System for Continuous Estimating and Monitoring Cardiac Output via Arterial Waveform Analysis,” *J. Biomed. Phys. Eng.*, vol. 7, no. 2, pp. 181–190, Jun. 2017.
- [39] A. Ben-Tal, S. S. Shamailov, and J. F. R. Paton, “Evaluating the physiological significance of respiratory sinus arrhythmia: looking beyond ventilation–perfusion efficiency,” *J. Physiol.*, vol. 590, no. 8, pp. 1989–2008, Apr. 2012.
- [40] N. R. A., W. Jijiang, B. Sunit, E. Cory, and M. David, “Respiratory Sinus Arrhythmia,” *Circ. Res.*, vol. 93, no. 6, pp. 565–572, Sep. 2003.
- [41] M. Elgendi, “On the analysis of fingertip photoplethysmogram signals,” *Curr. Cardiol. Rev.*, vol. 8, no. 1, pp. 14–25, Feb. 2012.
- [42] G. Joseph, A. Joseph, G. Titus, R. M. Thomas, and D. Jose, “Photoplethysmogram (PPG) signal analysis and wavelet de-noising,” in *2014 Annual International Conference on Emerging Research Areas: Magnetism, Machines and Drives (AICERA/ICMMD)*, 2014, pp. 1–5.
- [43] B. Escobar-Restrepo, R. Torres-Villa, and P. A. Kyriacou, “Evaluation of the Linear Relationship Between Pulse Arrival Time and Blood Pressure in ICU Patients: Potential and Limitations,” *Frontiers in Physiology*, vol. 9, p. 1848, 2018.